Journal of Molecular Structure 1060 (2014) 239–250

Contents lists available at ScienceDirect

Journal of Molecular Structure

journal homepage: www.elsevier.com/locate/molstruc

Study of the cyclodextrin and its complexation with 2,4-dinitrobenzoic acid through photophysical properties and 2D NMR spectroscopy

T. Stalin [a,*], K. Srinivasan [a], K. Sivakumar [b]

[a] School of Chemical Sciences, Department of Industrial Chemistry, Alagappa University, Karaikudi 630 003, Tamilnadu, India
[b] Department of Chemistry, Sri Chandrasekharendra Saraswathi Viswa Mahavidyalaya University, Enathur, Kanchipuram 631 561, Tamilnadu, India

HIGHLIGHTS

- Photophysical and electrochemical studies plays a major role in the host–guest inclusion complex process.
- Solid complex characterized by ^{1}H NMR, 2D NMR, FT-IR, XRD and SEM techniques.
- The structure of inclusion complex proposed by molecular docking study.

ARTICLE INFO

Article history:
Received 13 August 2013
Received in revised form 10 November 2013
Accepted 20 November 2013
Available online 28 December 2013

Keywords:
β-Cyclodextrin
2,4-Dinitrobenzoic acid
Patch dock server
2D ^{1}H NMR
ROESY

ABSTRACT

The host–guest inclusion complex formation of 2,4-dinitrobenzoic acid (2,4-DNB) with nano-hydrophobic cavity of β-cyclodextrin (β-CD) in solution phase were studied by UV–visible spectrophotometer and electrochemical method (cyclic voltammetry, CV). The prototropic behaviors of 2,4-DNB with and without β-CD and the ground state acidity constant (p*K*a) of host-guest inclusion complex (2,4-DNB-β-CD) was studied. The binding constant of the inclusion complex at 303 K was calculated using Benesi–Hildebrand plot. The solid inclusion complex formation between β-CD and 2,4-DNB was confirmed by ^{1}H NMR, 2D ^{1}H NMR (ROESY), FT-IR, XRD and SEM analysis. A schematic representation of this inclusion process is proposed by molecular docking studies using the patch dock server.

1. Introduction

Cyclodextrins (CDs) are cyclic oligosaccharides consisting of 6, 7, and 8 units of 1,4-linked glucose units, and are named alpha (α), beta (β) and gamma (γ)-Cyclodextrins, respectively (Scheme 1). These macromolecules, which can be spatially represented as a torus with wide and narrow openings corresponding to secondary and primary hydroxyl groups respectively, can encapsulate a large variety of compounds due to the hydrophobic character of their internal cavity [1]. Although the depth of the cavities for the three CDs is the same (~0.78 nm), their cavity diameters are ~0.57, 0.78 and 0.95 nm respectively (Scheme 1). Due to the unique chemical structure of CD molecules, the inner side of the cavity is hydrophobic and the outer side is hydrophilic. The hydrophobic nature of the CD cavities facilitates the ability of CDs to act as host for both non-polar and polar guests, which include small molecules as well as polymers [1–4]. Once the inclusion compound is formed, the stability of the guest molecules increases due to the binding forces (van der Waals attractions, hydrogen bonding, hydrophobic attractions, etc.) between the host (CDs) and guest molecules [5,6]. The CDs also have several advantages in other areas, such as the food, cosmetics industries and agro chemistry [7–9], especially owing to their capacity to protect the guest molecules against oxidation, light-induced reaction and loss by evaporation. Additionally, they usually enhance the aqueous solubility of poorly soluble or even insoluble compounds [10].

2,4-Dinitrobenzoic acid (2,4-DNB) belong to major organic pollutants that have been analysed in the environment. 2,4-DNB used as an anticorrosion protection of metals and or coated with a Cr-laminated glass support when mixed with cross linkable buthylmetacrylate and then heated under defined conditions. Aqueous emulsions of some dinitrobenzoic acids were used in order to render steel sheet and strip C-smut free after batch annealing [11]. 2,4-DNB are listed as priority pollutions by the US Environmental Protection Agency [12]. They have great potential toxicities of carcinogenesis, teratogenesis, and mutagenesis [13,14]. It's released into the air, water and soil. It may also be released into the environment from landfill leaks and accidental spills. Consequently, due to the harmful effects of these organic compounds, the

* Corresponding author. Tel.: +91 9944266475; fax: +91 4565 225202.
E-mail addresses: drstalin76@gmail.com, tstalinphd@rediffmail.com (T. Stalin).

0022-2860/$ - see front matter © 2013 Elsevier B.V. All rights reserved.
http://dx.doi.org/10.1016/j.molstruc.2013.11.048

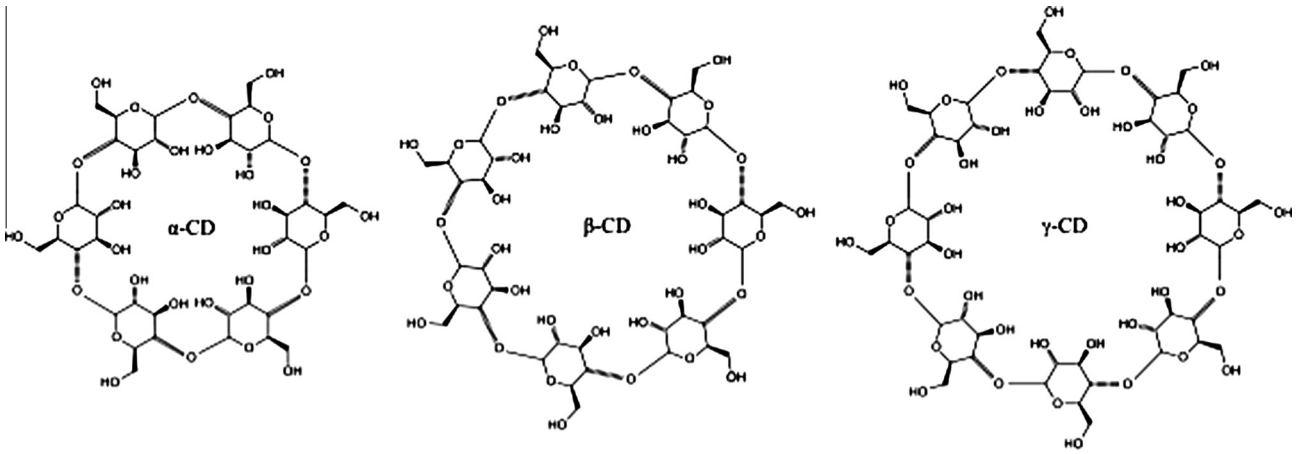

Scheme 1. 3D view of chemical structures of α-CD, β-CD and γ-CD.

wastewaters containing them must be treated before being discharged to receiving water bodies. In order to assess the fate of 2,4-DNB in wastewater and to control their mobility and reactivity during remediation processes, the sorption behavior of these toxic contaminants must be understood and revealed.

The author studied the host-guest inclusion complex mechanism between 2,4-DNB and β-CD in different techniques. In this study, we report for the spectral and electrochemical behaviors of 2,4-DNB in different pH with β-cyclodextrin. With respect to the formation of host-guest inclusion complex of 2,4-DNB with β-CD in solution phase was studied by UV–Visible spectroscopy (UV–Vis) and cyclic voltammetric technique (CV). The solid complex was prepared and characterized by ^{1}H NMR, 2D ^{1}H NMR (ROESY), FT-IR, XRD, and SEM techniques. The schematic representation of this inclusion process is proposed by molecular docking studies using the patch dock server.

2. Experimental

2.1. Instruments

The UV–Vis spectra (absorption spectral measurements) were carried out with Shimadzu UV-2401PC double-beam spectrophotometer (range 1100–200 nm) with scan speed of 400 nm min^{-1}, the pH values in the range 1.0–12.0 were measured on Elico pH meter LI-120; Electrochemical studies were carried out using Auto lab electrochemical analyzer (GPES software), A conventional three electrode cell assembly was used for the electrochemical measurements. Cyclic Voltammetry measurements at a glassy carbon electrode (diameter: 1 mm) were carried out at an applied potential of −0.9 V to 0.4 V for each concentration of β-cyclodextrin at single cycle only. Reference electrode was saturated calomel electrode (SCE) and platinum wire as counter electrode. All experiments were carried out at 30 ± 1 °C. The working electrode was polished to a mirror with 0.05 μm alumina aqueous slurry, and rinsed with triply distilled water before each experiment. The supporting electrolyte was pH∼1 (0.1 M H_2SO_4 + 0.1 M Na_2SO_4) and pH∼7 (0.1 M KH_2PO_4 + 0.1 M NaOH). FT-IR was recorded using Nicolet 380 Thermo Electron Corporation Spectrophotometer using KBr pellets and scan between 4000 and 400 cm^{-1}. The sample solutions for ^{1}H NMR were prepared by dissolving the dinitro compounds and their complexes in D_2O solvent to obtain the final concentration of 20 mM. Two-dimensional rotating-frame Overhauser effect spectroscopy (ROESY) experiments were performed using BRUKER-NMR 400 MHz instrument operating at 300 K and the standard Bruker program was used, DMSO-d_6 was used as a solvent, relaxation delay of 1 s and mixing time 300 ms under the spin lock conditions. Powder X-ray diffraction spectra were taken by XPert PRO PANalytical diffractometer (2Theta:0.001; Minimum step size Omega:0.001). The surface morphology was taken by Hitachi S 3000 H SEM.

2.2. Molecular docking study

The most probable structure of the 2,4-DNB:β-CD inclusion complex was determined also by molecular docking studies using the Patch Dock server [15]. The 3D structural data on β-CD was obtained from HIC-Up database (http://xray.bmc.uu.se/hicup) using the search interface. The 3D structures of 2,4-DNB were obtained by translating the SMILES formula of 2,4-DNB using CORINA server (http://www.molecular-networks.com/ online_demos/corina_demo).The guest molecule (2,4-DNB) was docked into the host molecule (β-CD) cavity using PatchDock server by submitting the 3D coordinate data of 2,4-DNB and β-CD molecules. Docking was performed with complex type configuration settings. PatchDock server follows a geometry-based molecular docking algorithm to find the docking transformations with good molecular shape complementary. PatchDock algorithm separates the Connolly dot surface representation [16] of the molecules into concave, convex and flat patches. These divided complementary patches are matched in order to generate candidate transformations and evaluated by geometric fit and atomic desolvation energy scoring [17] function. RMSD (root mean square deviation) clustering is applied to the docked solutions to select the non-redundant results and to discard redundant docking structures.

2.3. Reagents

β-Cyclodextrin {(β-CD), were obtained from the Sd fine chemical company} and used without further purification. 2,4-Dinitrobenzoic acid (2,4-DNB) purchased from Alfa Aesar company and used without further purification. Triply distilled water was used to prepare all solutions. Solutions in the pH range 2.0–12.0 were prepared by adding the appropriate amount of NaOH and H_3PO_4. Yagil basicity scale (H_-) [18] for solutions above pH∼12 (using a NaOH–H_2O mixture) and a modified Hammett's acidity scale (H_0) [19] for the solutions below pH∼2 (using a H_2SO_4–H_2O mixture) was employed. The solutions were prepared just before taking measurements. The concentrations of the solutions were of the order (10^{-4} to 10^{-5} mol dm^{-3}). The stock solution of 2,4-DNB and β-CD preparation for spectral and electrochemical studies was

Table 1
Various prototropic maxima (absorption spectra) and p*K*a values of 2,4-DNB in without and with β-CD medium.

Species	Without β-cyclodextrin		With β-cyclodextrin	
	λ_{max} (nm)	H_0/pH/H_	λ_{max} (nm)	H_0/pH/H_
Monocation	310(Sh)	1	310(sh)	1
	243		241	
Neutral	255	2.0–15.4	252	2.0–15.4
	208		207	
Monoanion	421	15.62	421	15.62
	290		290	
	219		219	
p*K*a		1.4		1.18

[a] Sh-Shoulder.

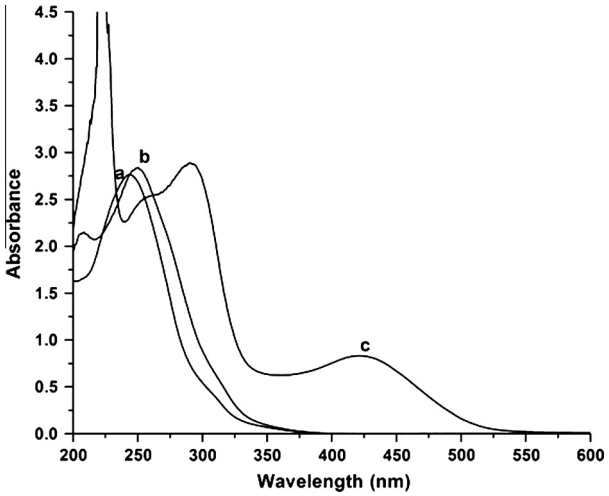

Fig. 1. Absorption spectra of different prototropic species of 2,4-DNB at 303 K; concentration 2×10^{-4} M (a) monocation, (b) neutral and (c) monoanion.

prepared by adopting the procedure detailed in our previous report [20,21].

2.4. Preparation of solid inclusion complex of 2,4-DNB with β-CD

Accurately weighed 1 g of the β-CD was placed into 50 ml conical flask and 30 ml triply distilled water added and then oscillated this solution enough. After that, 0.1628 g 2,4-DNB was put into a 50 ml beaker and 20 ml ethanol added and put over electromagnetic stirrer to stir until it was dissolved [22]. Then slowly poured 2,4-DNB solution into β-CD solution. The above mixed solution was continuously stirred for 48 h at room temperature. The reaction mixture was put and kept in refrigerator for 48 h. At this time, we observed that yellow precipitate is formed. The precipitate was filtered by G4 crucible and washed with triply distilled water. The precipitate is taken in a Petri dish and spread over as thin layer and then dried in oven at 50 °C for 12 h. After drying in the oven the yellow powder was obtained. This is solid inclusion complex of 2,4-DNB with β-CD and it further analyzed by ^{1}H NMR, 2D ^{1}H NMR (ROESY), FT-IR, XRD and SEM analysis.

3. Results and discussion

3.1. Effect of pH

The absorption of 2,4-DNB has been studied in the different pH range and the relevant data are compiled in Table 1 and Fig. 1. There are three prototropic species (monocation, neutral, and monoanion) present in the prototropic behavior of this molecule. In the pH range of 2 to H_15.4, the absorption maxima (255 nm) resemble the spectra observed in non-aqueous solvents (e.g. in 2-Propanol at 240 nm, and 1,4-Dioxane at 243 nm, Ethyl acetate 254 nm) and thus can be assigned to the neutral species (Fig. S1 and Table S1) in these pH ranges. Above H_15.4 the absorption spectrum of 2,4-DNB is red shifted in comparison to the neutral species and is assigned to monoanion formed by deprotonating the carbonyl (—COOH) group (290 and 421 nm). A further increase in the base strength, which is no change in the absorption maxima in comparison to monoanion, hence there is no possibility to form a dianion in this molecule. When acid concentration is increased from pH∼2, the absorption maxima of 2,4-DNB is red shifted in the absorption maximum of 310 nm (shoulder peak) but another one absorption peak observed at 243 nm. This spectrum is clearly indicated that protonation should occur at the carbonyl group. Here a progressive shift with an increase in the concentration of acid and at pH∼1.0 a UV band appears due to the formation of monocation. If π–π^* transition is the lowest energy transition, protonation of carbonyls results in a red shift of the electronic spectrum. As mentioned earlier, π–π^* is the lowest energy transition in 2,4-DNB. The red shift confirms the formation of the cation on protonation of the carbonyl group. However, in the ground state, a red shift is observed in neutral and monoanion, this behavior is different from its monocation. Further the p*K*a value of the monocation-neutral and neutral-monoanion equilibrium (p*K*a) values is calculated by spectrophotometric methods (Table 1). The prototropic equilibrium is shown in Scheme 2.

3.2. Effect of β-cyclodextrin

Table 2 and Fig. 2 show the absorption maxima of 2,4-DNB in pH∼1.0 (monocation) and pH∼7 (neutral) solutions containing

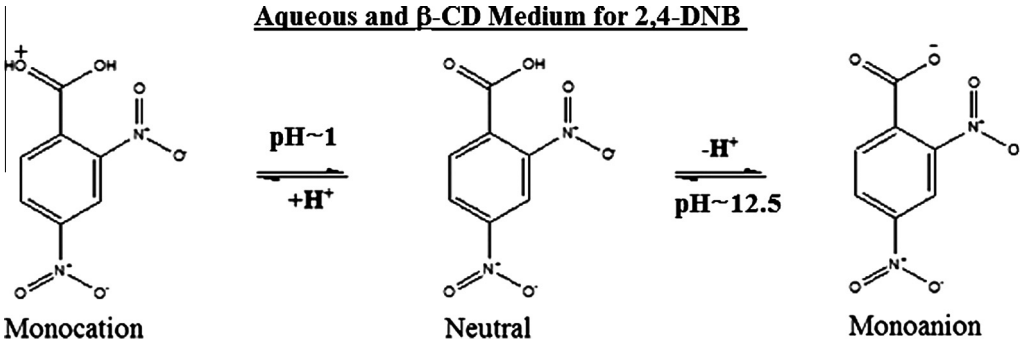

Scheme 2. Prototropic equilibria of 2,4-DNB in aqueous and β-CD medium.

Table 2
Absorption maxima (nm) and log ε of 2,4-DNB at different concentrations of β-CD in pH∼1 and pH∼7 solutions.

S. No	Concentration of β-CD (M)	pH∼1		pH∼7	
		λ_{max} (nm)	log ε	λ_{max} (nm)	log ε
1	0	310 sh 243	3.23 4.2	310sh 250 208	3.5 4.2 4
2	0.002	310sh 242	3.29 4.2	310sh 249 207	3.52 4.2 4
3	0.004	310sh 242	3.32 4.2	310sh 249 207	3.54 4.2 4
4	0.006	310sh 241	3.38 4.2	310sh 249 207	3.55 4.2 4
5	0.008	310sh 241	3.42 4.2	310sh 248 207	3.56 4.2 4
6	0.01	310sh 241	3.44 4.2	310sh 248 207	3.57 4.2 4
7	0.012	310sh 241	3.48 4.2	310sh 248 207	3.58 4.2 4
Binding constant (M^{-1})		92		152	
ΔG (kJ/mol)		−11.4		−12.7	

Sh-shoulder.

different concentrations of β-CD. At pH∼7, 2,4-DNB exists as a neutral form only, hence we also recorded spectra at pH∼1.0 cationic form. The absorption spectra of these two forms (neutral, monocation) are drastically different. In pH∼7 and pH∼1.0 no clear isosbestic point was observed in the absorption spectra even in the presence of higher β-CD concentration. The equilibrium between neutral and monocation forms of 2,4-DNB in β-CD medium.

$$\beta\text{-CD} : 2,4\text{-DNBH}^{+} \underset{+H^{+}}{\overset{pH\sim1.5}{\rightleftharpoons}} \beta\text{-CD} + 2,4\text{-DNB} \overset{pH\sim7}{\rightleftharpoons} \beta\text{-CD} : 2,4\text{-DNB} \quad (1)$$

In pH∼7 solution the absorption maxima is increased and 1:1 inclusion complex was formed, whereas the absorption spectra of 2,4-DNB in pH∼7 there was a blue shift (250 nm to 248 nm) in the absorption maxima and also the absorption intensity was increased with increasing the β-CD concentration. In pH∼7 the 2,4-DNB located inside the β-CD cavity and the COOH group located at above the β-CD rim, which will cause the increase of the absorbance. In pH∼1.0; 2,4-DNB exist as a cationic form with 1:1 inclusion complex form, In pH∼1.0 the 2,4-DNB located inside the β-CD cavity and the $COOH_2^+$ group located in the β-CD rim. This behavior has been attributed to the enhanced dissolution of the 2,4-DNB molecule through the hydrophobic interaction between 2,4-DNB and β-CD. These results indicate that 2,4-DNB molecule is entrapped into β-CD cavity to form an inclusion complex. In both cases, the binding constant for the formation of 2,4-DNB: β-CD complex has been determined by analyzing the changes in the intensity of absorbance with the β-CD concentration. Fig. 3 plotting $1/(A-A_0)$ versus $1/[\beta\text{-CD}]$ for a 1:1 host:guest inclusion complex. In 1:1 inclusion complex gives straight line at pH∼7, and pH∼1.0, The binding constant (K) can be obtained by using the modified Benesi–Hildebrand equation [23] for the 1:1 complex Eq. (2) between 2,4-DNB and β-CD as shown below.

$$\frac{1}{A-A_0} = \frac{1}{\Delta\varepsilon[G]_0[H]_0K} + \frac{1}{\Delta\varepsilon[H_0]} \quad (2)$$

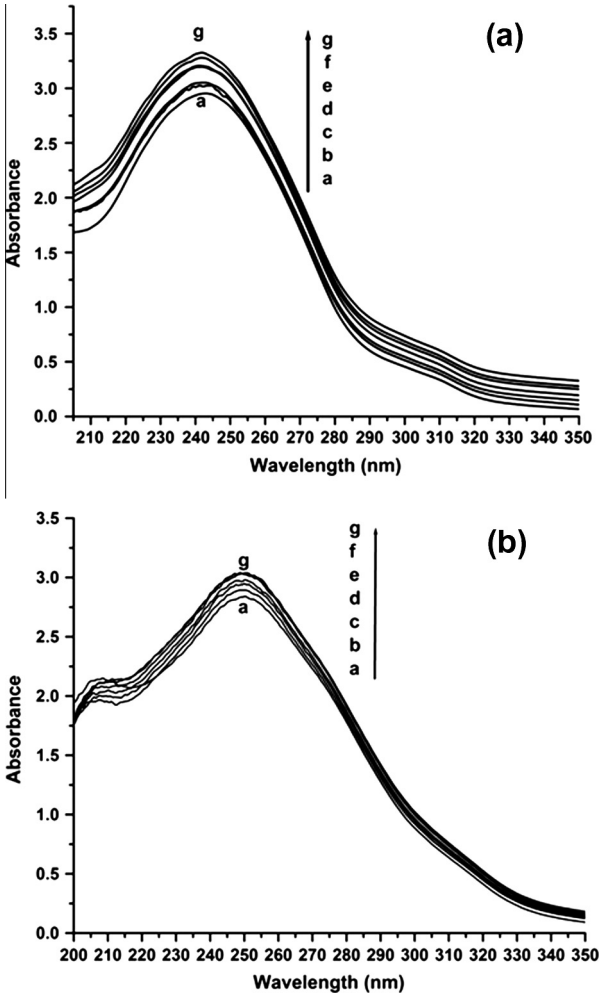

Fig. 2. Absorption spectra of 2,4-DNB (Conc.2 × 10^{-4} M) in (a) pH∼1 and (b) pH∼7 solution at different β-CD (a–g Conc. 0–12 × 10^{-3} M).

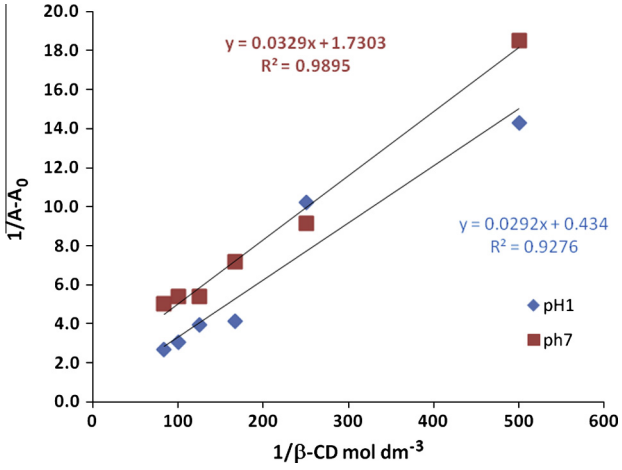

Fig. 3. Benesi-Hildebrand plot of $1/A-A_0$ Vs $1/[\beta\text{-CD}]$ for 2,4-DNB in pH∼1 and pH ∼7 solution.

where $A-A_0$ is the difference between the absorbance of 2,4-DNB in the presence and absence of β-CD, $\Delta\varepsilon$ is the difference between the molar absorption coefficient of 2,4-DNB and the inclusion complex, where $[G]_o$ is $[2,4\text{-DNB}]_0$ and $[H]_o$ is $[\beta\text{-CD}]_0$ are the initial concentration of 2,4-DNBand β-CD, respectively. A good correlations were

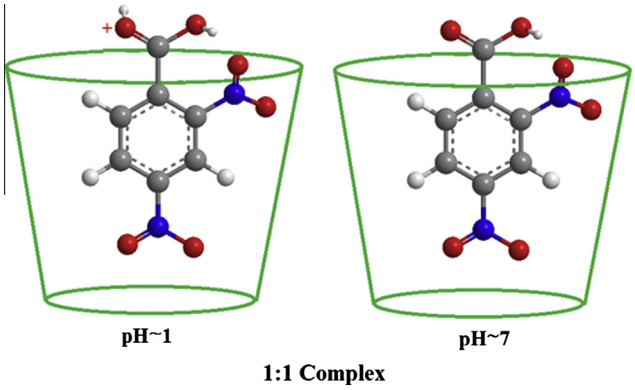

Scheme 3. The proposed structure of inclusion complex of 2,4-DNB with β-CD for 1:1 inclusion complex. The oxygen atoms are shown as red ball, nitrogen as blue and carbon as gray colour balls; hydrogen atoms are white balls. (For interpretation of the references to colour in this figure legend, the reader is referred to the web version of this article.)

obtained for pH∼7 and pH∼1 respectively (Fig. 3; r^2 = 0.9864 and 0.978), confirm that the formation of 1:1 inclusion complexes. From the intercept and slope values of this plot *K* were calculated [pH∼1 = 92 M^{-1}, pH∼7 = 152 M^{-1}] at 303 K (Table 2).

3.3. Possible inclusion complex of 2,4-DNB with β-CD cavity

The absorption spectra of 2,4-DNB have been studied in the pH range 1 to H_15.4 in β-CD (Table 1). When compared with aqueous medium no appreciable change is observed in β-CD in absorption maxima of neutral and monocation. The ground state p*K*a values for the neutral-monocation equilibrium are also same. Considering the above discussions, the possible inclusion mechanism is proposed as follows. Naturally, two different types of inclusion complex formation between 2,4-DNB and β-CD are possible. In pH∼1, the carbonyl group is protonated, moreover it available in the near of the upper rim of the β-CD by the cationic charge structure (Scheme 3). In pH∼7, the carboxyl group of 2,4-DNB is not protonate or deprotonate in the β-CD solution. This is indicated in the neutral molecule absorption maxima of 2,4-DNB is red shifted in β-CD than protonated form. The ground state p*K*a values for the neutral-monocation equilibrium are listed in Table 1. This confirms that the environments around the COOH in β-CD are same in the bulk aqueous medium and OH group present in the β-CD cavity. These features indicate that the probable inclusion complex structure represented in the Scheme 3. This is further supported by using semi empirical quantum mechanical calculations discussed in Section 3.4. To substantiate the above discussion, the effect of β-CD on the prototropic equilibrium, the 2,4-DNB was present as monocation in pH 1.0, neutral in the pH range 2.0–15.4 and the prototropic equilibrium molecular resonance structure can be written in the Scheme 2. These results indicate that 2,4-DNB molecule is entrapped into the β-CD cavity to form a 1:1 inclusion complex.

3.4. Semi empirical quantum mechanical calculations

The internal diameter of the β-CD is approximately 6.5 Å and its height is 7.8 Å (Scheme 4). Considering the shape and dimensions of β-CD, the ground state of 2,4-DNB molecules were optimized using AM1 method (Scheme 4). In 2,4-DNB, the vertical distances between H_{19}—O_{14} is 8.3 Å and H_{19}—O_{15} is 8.0 Å. The horizontal distance between H_{18}—O_1 is 5.0 Å and H_{18}—O_3 is 5.6 Å. The vertical distance and the horizontal distance measured from the terminal atoms of 2,4-DNB are less than the height and vertical diameter of β-CD. Since, the height of 2,4-DNB are lower than that of β-CD, the insertion of 2,4-DNB in the β-CD cavity is possible as shown in Scheme 3.

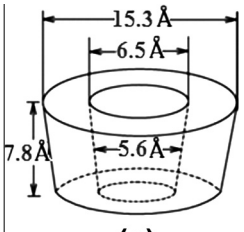

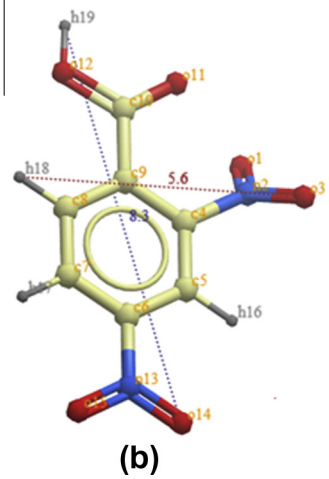

2,4-DNB bond distance in Å		Orientation
H_{19} - O_{14}	8.3	Vertical
H_{19} - O_{15}	8.0	Vertical
H_{18} - O_1	5.0	Horizonal
H_{18} - O_3	5.6	Horizonal

Scheme 4. Schematic representation of semi empirical bond distance of (a) β-CD and (b) 2,4-DNB.

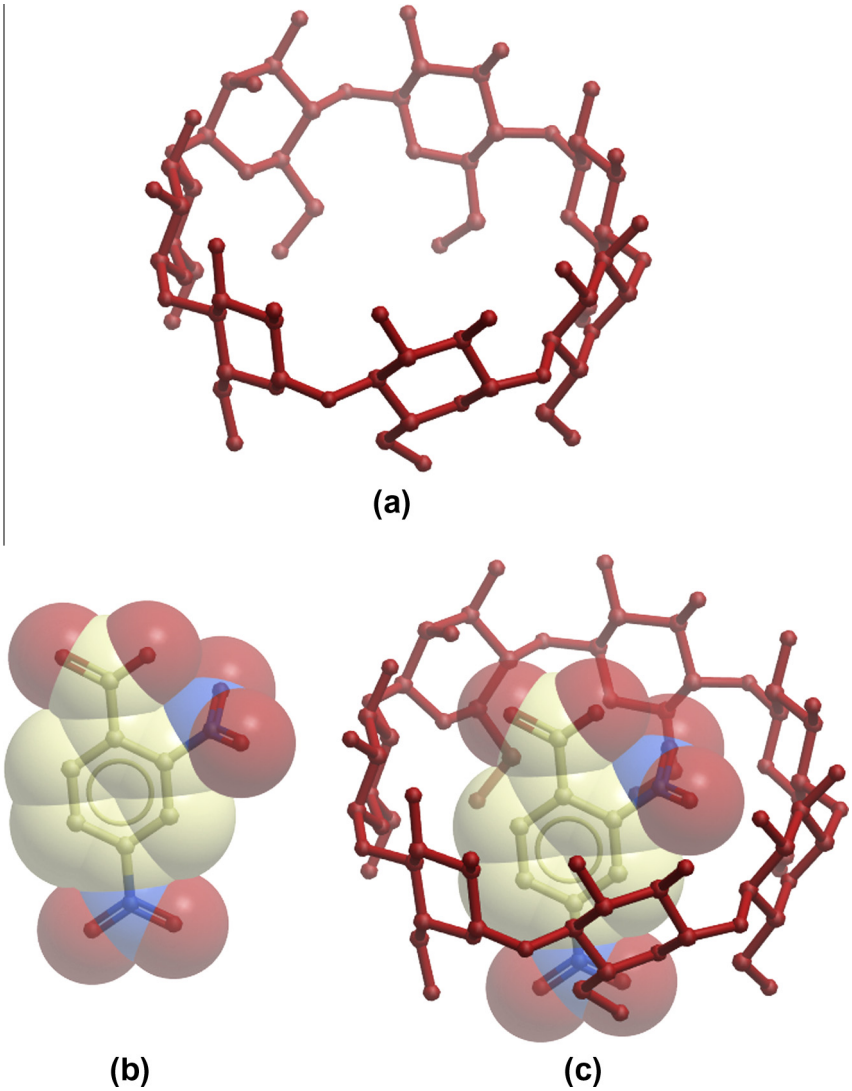

Scheme 5. Ball and stick representation of (a) β-CD, (b) 2,4-DNB, (c) 2,4-DNB:β-CD inclusion complex; the oxygen atoms are shown as red ball, nitrogen as blue and carbon as grey balls; hydrogen atoms are white balls. (For interpretation of the references to colour in this figure legend, the reader is referred to the web version of this article.)

3.5. Molecular docking studies of inclusion process

The 3D structure of β-CD, 2,4-DNB was obtained from crystallographic databases are shown in Scheme 5(a and b). The guest molecules of 2,4-DNB were docked into the cavity of β-CD using PatchDock server. The PatchDock server program gave several possible docked models for the most probable structure based on the energetic parameters; geometric shape complementarity score, approximate interface area size and atomic contact energy of the 2,4-DNB:β-CD inclusion complexes. The docked 2,4-DNB:β-CD 1:1 model Scheme 5c with the highest geometric shape complementarity score 2500 for 2,4-DNB:β-CD, the approximate interface area size of 2,4-DNB:β-CD was 266.2 $Å^2$ and atomic contact energy of −861 kJ/mol for the inclusion complex of 2,4-DNB:β-CD was calculated. This is highly probable and energetically favorable model and it was in good correlation with results obtained through experimental methods.

3.6. Electrochemical studies

The cyclic voltammograms shows an electrochemical behavior of 2,4-DNB in pH∼1 and pH∼7 with β-CD (Fig. 4 and Table 3). Formation of the inclusion complex of 2,4-DNB with β-CD was also confirmed by electrochemical method. In pH∼7 the cyclic voltammograms shows an anodic peak during the forward scan (towards positive potential) at 0.058 V and two reduction peaks during the reverse scan (towards negative potential) at −0.198 V and −0.855 V. These peaks are ascribed as oxidation of 2,4-DNB (COOH; 0.058 V) and the reduction of carboxyl cation (−0.198 V) into COOH and another one reduction peak of NO_2 (−0.855 V) into hydroxylamine.

In pH∼1, from the cyclic voltammograms one oxidation peak during the forward scan (towards positive potential) at 0.329 V and two-reduction peaks were observed during the reverse scan (towards negative potential) at 0.283 V and −0.415 V. These peaks were ascribed as oxidation of carboxyl cation into carboxyl group (0.329 V) and reduction of carboxyl group into carboxyl cation (0.283 V) and NO_2 (−0.415 V) into hydroxylamine. The oxidation and reduction mechanism of 2,4-DNB was clearly explained in Scheme 6.

The cathodic peak current (Fig. 4 and Table 3) i_{pc}, increased with increasing the β-CD concentration in both pH solutions (pH∼1.5 and pH∼7). The cathodic peak potential, Ep_c, shifted towards a positive direction in pH∼7 and negative direction in pH∼1.5 when

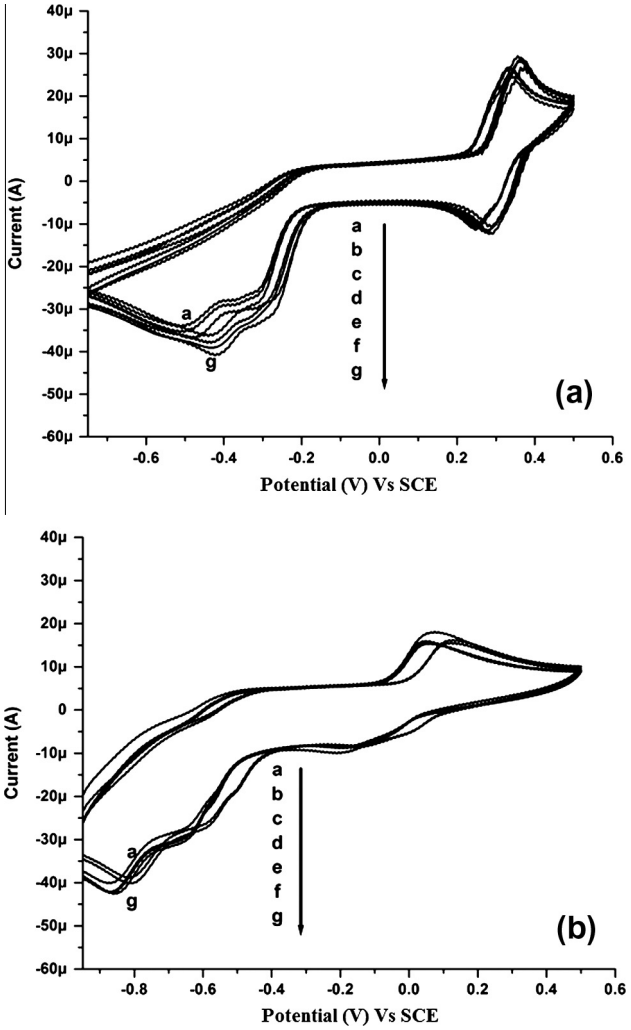

Fig. 4. CV for 2,4-DNB:β-CD in pH∼1 and pH∼7 buffer solution, scan rate 100 mV s^{-1}, 2,4-DNB (Conc. 2 × 10^{-4} M) and β-CD (a–g Conc. 0–12 × 10^{-3} M).

β-CD concentration was increased in both cases. The result showed that the inclusion complex between 2,4-DNB and β-CD was formed when 2,4-DNB was added onto β-CD aqueous solution. In addition, the cathodic peak current was increased with increasing β-CD concentration; this is due to the nitro groups are encapsulated in the β-CD cavity and the catalytic behavior of β-CD to the included guest molecule (2,4-DNB).

The binding constant (K) and the stoichiometric ratio of the inclusion complex of 2,4-DNB can be determined according to the Benesi–Hildebrand [23] relation assuming the formation of a 1:1 host–guest complex.

$$\frac{1}{I_{HG}-I_G}=\frac{1}{\Delta I}+\frac{1}{K[2,4\text{-DNB}]_0\Delta I[\beta\text{-CD}]_0} \quad (3)$$

where I_G is the reduction peak current of the guest molecule of 2,4-DNB, and I_{HG} is the reduction peak current of the inclusion complex of 2,4-DNB:β-CD. $I_{HG}-I_G$ is the difference between the reduction peak current of inclusion complex and 2,4-DNB. ΔI is the difference between the molar peak current coefficient of the inclusion complex and 2,4-DNB. The $[2,4\text{-DNB}]_0$ and $[\beta\text{-CD}]_0$ are the initial concentration of 2,4-DNB and β-CD, respectively. Plot of $[1/I_{HG}-I_G]$ versus $1/[\beta\text{-CD}]$ gives a straight line for both pH solutions as shown in Fig. 5. Good linear correlations were obtained (r = 0.950, 0.923 for pH∼1 and pH∼7 respectively), confirm that the formation of a 1:1 inclusion complex for both pH (pH∼1 and pH∼7) solutions. From the intercept and slope values of this plot K was evaluated, the binding constant values for 2,4-DNB:β-CD is 38 $M^{-1}$and 83 M^{-1} in pH∼1 and pH∼7 respectively. These values indicate that 2,4-DNB molecule is encapsulated in the β-CD cavity to form an inclusion complex.

3.7. ^1H NMR spectrum

The formation of the solid inclusion complex can be analyzed from ^{1}H NMR spectra [24]. Fig. 6; Tables 4 and 5 showed the typical ^{1}H NMR spectra of (a) β-CD, (b) the solid inclusion complex of 2,4-DNB with β-CD (chemical shift changes with β-CD), (c) 2,4-DNB and (d) the solid inclusion complex (chemical shift changes with 2,4-DNB). The significant distinguish for these ^{1}H NMR spectra strongly confirmed that the solid inclusion complex formation. The values of chemical shifts, δ for different protons in β-CD with solid inclusion complex and 2,4-DNB with solid inclusion complex were listed in Tables 4 and 5. It can be seen from the ^{1}H NMR that in solid inclusion complex, a great upfield shift was occurring for H_3 and H_5 protons, which locate in the nano hydrophobic cavity of β-CD (Scheme 7b). The changes of chemical shift ($\Delta\delta$) of H_3 and H_5 suggested that the 2,4-DNB monomer completely entered into the nano hydrophobic cavity of β-CD. The phenyl ring of 2,4-DNB made the signals of β-CD protons (H_3 and H_5) upfield shift. On the contrary, the chemical shifts of H_1,

Table 3
CV for 2,4-DNB:β-CD in pH∼2 and pH∼7 buffer solution, scan rate 100 mV s^{-1}, 2,4-DNB (Conc. 2 × 10^{-4} M) and (a–g) 0–12 × 10^{-3} M β-CD concentrations.

Concentration of β-CD (M)	pH∼1				pH∼7			
	Epa (V)	Ipa (μA)	Epc (V)	Ipc (μA)	Epa (V)	Ipa (μA)	Epc (V)	Ipc (μA)
0	0.329	13.89	0.283	−14.63	0.058	9.461	−0.198	−0.375
			−0.498	−20.24			−0.804	−7.49
0.002	0.334	14.63	0.283	−16.21	0.044	9.346	−0.191	−0.473
			−0.489	−21.06			−0.804	−5.462
0.004	0.334	15.27	0.293	−17.29	0.049	8.89	−0.149	−3.685
			−0.474	−22.66			−0.85	−7.968
0.006	0.356	15.33	0.29	−16.4	0.051	8.628	−0.152	−3.585
			−0.43	−23.57			−0.85	−5.322
0.008	0.356	15.63	0.249	−17.5	0.063	8.614	−0.176	−3.629
			−0.423	−23.69			−0.855	−5.084
0.01	0.363	16.15	0.254	−18.64	0.122	8.221	−0.108	−3.322
			−0.41	−23.98			−0.855	−5.582
0.012	0.366	16.45	0.254	−19.29	0.117	8.611	−0.142	−1.624
			−0.415	−25.26			−0.857	−5.997
Binding constant (M^{-1}).	38				83			
ΔG (kJ/mol)	−9.2				−11			

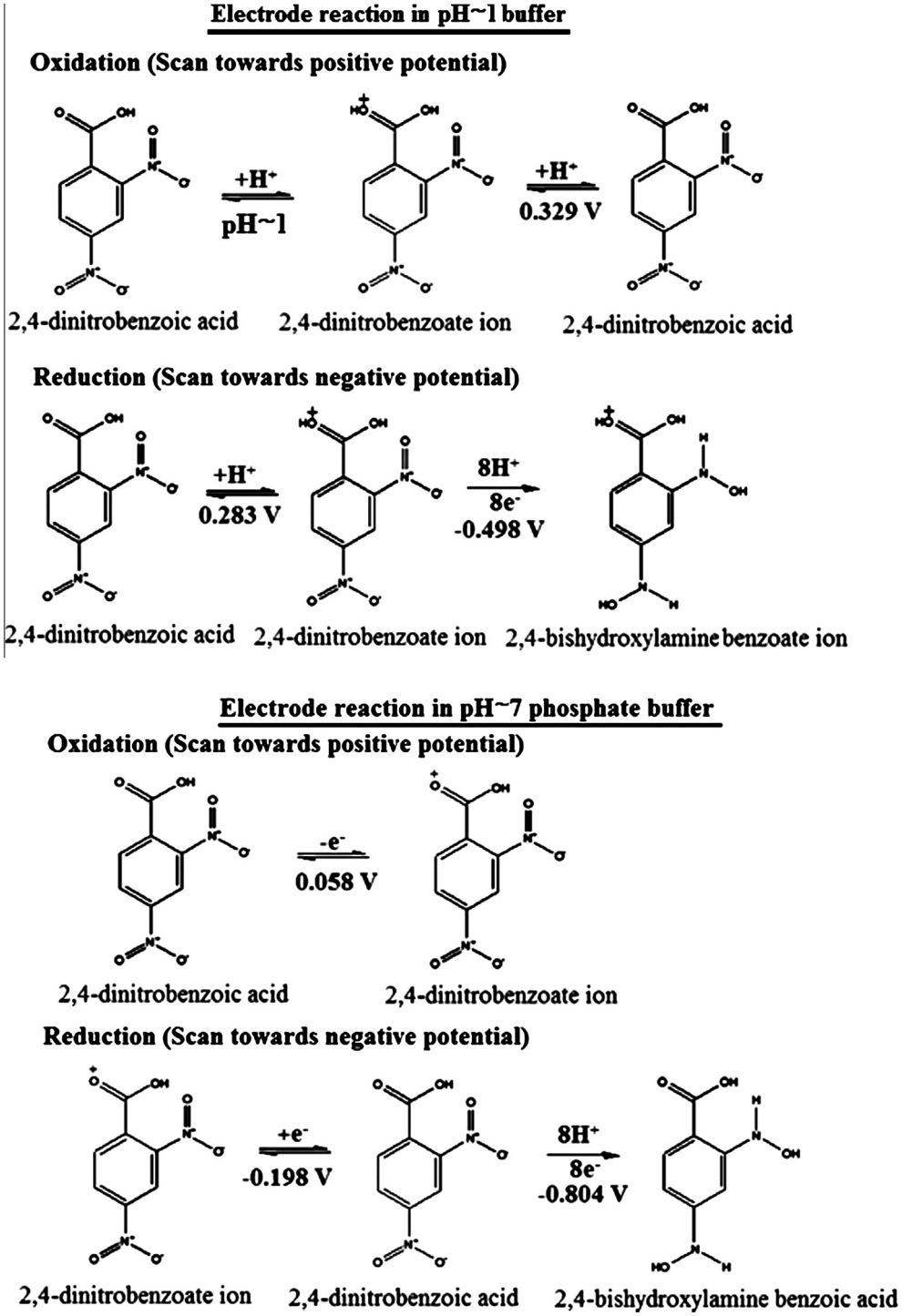

Scheme 6. Reaction mechanism of 2,4-DNB in pH∼1 and pH∼7 buffer solution at glassy carbon electrode.

H_2, H_4, and H_{6ab}, which are on the outer surface of β-CD and the narrow opening of β-CD as shown as in Scheme 7b, were only slightly affected by the guest molecule. Similarly, the chemical shifts of H_a, H_b and H_c of 2,4-DNB (Scheme 7c) are located in the nano hydrophobic cavity of β-CD was also moved in upfield significantly because the interaction between 2,4-DNB and β-CD. On the other hand, as shown as in Fig. 6d, when 2,4-DNB monomer entered into the nano hydrophobic cavity of β-CD, the change of the micro-environment of 2,4-DNB protons leaded the phenyl ring protons moved upfield shift. From the above discussions we can conclude that of 2,4-DNB molecule was included into nano hydrophobic cavity of β-CD.

3.7.1. 2D ^{1}H NMR (ROESY) studies on 2,4-DNB with β-CD

The 2D ^{1}H NMR (ROESY) is a powerful technique for investigation of inter and intra molecular interactions. The chemical shift changes were shown by H_a, H_b and H_c protons of aromatic (hydrophobic part) moiety [25] of dinitrophenol may play a major role in the inclusion process. To verify this hypothesis, 2D ^{1}H NMR (ROESY) spectra were recorded. The presence of NOE cross-peaks

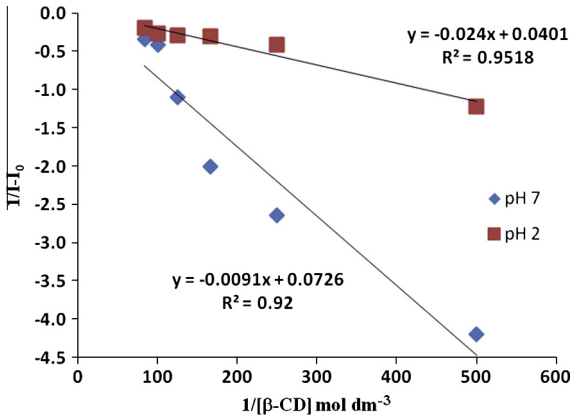

Fig. 5. Benesi–Hildebrand plot of $1/I_{HG} - I_G$ vs. 1/[β-CD] for 2,4-DNB in pH∼1 and pH∼7 solution.

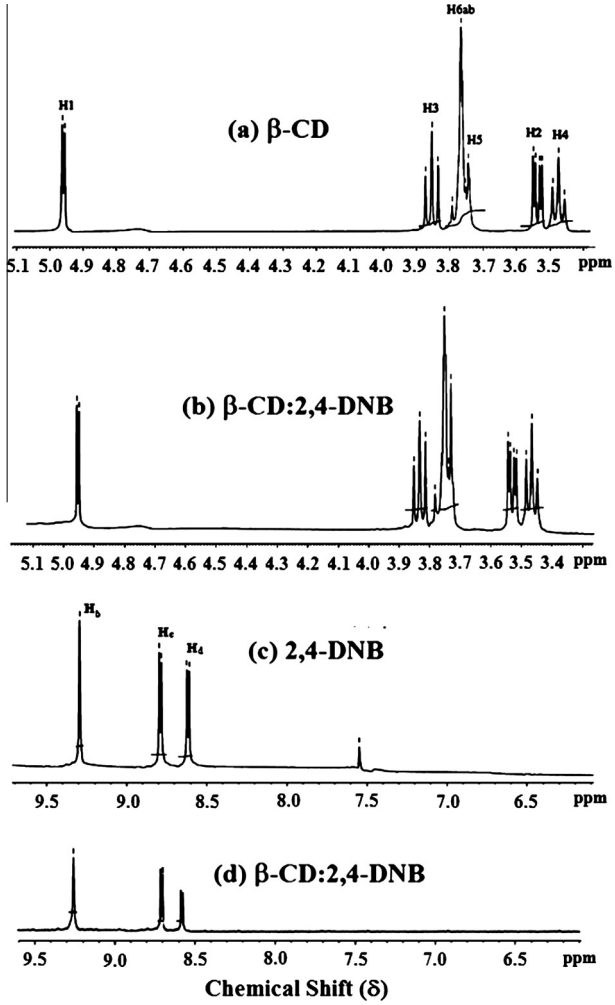

Fig. 6. ^{1}H NMR spectra of (a) β-CD, (b) the solid complex (chemical shift with respect to β-CD), (c) 2,4-DNB and (d) the solid complex (chemical shift with respect to 2,4-DNB).

between protons of two different species in the 2D ^{1}H NMR spectrum is an indication that they are in spatial contact through space within the cavity of β-CD.

Fig. 7 shows the 2D spectrum of (a) 2,4-DNB:β-CD and (b) counterpart of 2,4-DNB: β-CD systems, two groups of intermolecular NOE cross-peaks were observed. In the complex of 2,4-DNB:β-CD,

Table 4
^{1}H NMR chemical shifts of β-CD in free and complexed state determined in D_2O at 303 K.

Proton	β-CD δ (ppm)	2,4-DNB-β-CD δ (ppm)	Δδ
H_1	4.966	4.963	−0.003
H_2	3.554	3.553	−0.001
H_3	3.877	3.862	−0.015
H_4	3.478	3.476	−0.002
H_5	3.748	3.735	−0.013
H_6	3.797	3.796	−0.001

Table 5
^{1}H NMR chemical shifts of 2,4-DNB in free and complexed state determined in D_2O at 300 K.

Proton	2,4-DNB δ (ppm)	2,4-DNB-β-CD δ (ppm)	Δδ
H_b	9.310	9.265	−0.045
H_c	8.810	8.786	−0.024
H_d	8.654	8.585	−0.069

the first peak was assigned to the interaction between the H_3 protons of β-CD with ortho positioned protons of the 2,4-DNB and other peak were assigned to the interaction between the H_5 protons of β-CD with meta positioned protons of the 2,4-DNB. In all cases the interaction of 2,4-DNB with only internal protons of the β-CD were observed. In addition the H_{6ab} protons of the β-CD were not affected by the inclusion process. We confirmed that the 2,4-DNB is included into the β-CD cavity via wider rim. From the above fact the 2,4-DNB interacts with β-CD through space contact, not by bonding.

3.8. FT-IR spectral studies

FT-IR is a very useful analytical tool to prove the existence of both guest and host molecules in their solid inclusion complex [26]. Fig. 8 shows the FT-IR spectra of the (a) 2,4-DNB, (b) β-cyclodextrin and (c) solid complex of 2,4-DNB and β-cyclodextrin. The FT-IR spectrum of the solid complex is almost similar to the β-cyclodextrin molecule. It indicates the formation of the solid inclusion complex, similar to an observation noticed by the same authors [20,21]. Besides that, a broad hydroxyl band of β-cyclodextrin at 3371 cm^{-1} appeared in the FT-IR spectrum of the solid inclusion complex which is a good evidence of the formation of the solid complex.

The wave number for the β-CD observed at 3371 cm^{-1}, 2929 cm^{-1}, 1158 cm^{-1}, and 1030 cm^{-1} which correspond to the symmetric and anti-symmetric stretching of OH, CH_2, C—C and bending vibration of O—H frequencies. Meanwhile the frequencies for 2,4-DNB were observed at 1531 cm^{-1}, 1350 cm^{-1}, 1722 cm^{-1}, 835 cm^{-1} and 1618 cm^{-1} in the respective functional groups such as NO_2, COOH, C—N and vibrational stretching of —C=C— respectively.

The solid complex formation has been verified by comparing the spectra of β-CD and 2,4-DNB (Fig. 8a and b), because the bands resulting from the included part of the guest molecule generally shifted or their intensities altered [26]. From Fig. 8 the characteristic stretching bands of $-NO_2$ are observed at 1531 cm^{-1} and 1350 cm^{-1} for 2,4-DNB were observed and these bands are shifted to 1544 cm^{-1}, 1352 cm^{-1} and the intensity of the bands are also reduced because the nitro groups were present (included) in the nanocavity of β-CD. The characteristic peak of the COOH stretching band appeared at 1722 cm^{-1} for 2,4-DNB and it shifted to 1726 cm^{-1} and also the intensity of the peak was reduced; due to the phenyl-COOH group are present in the

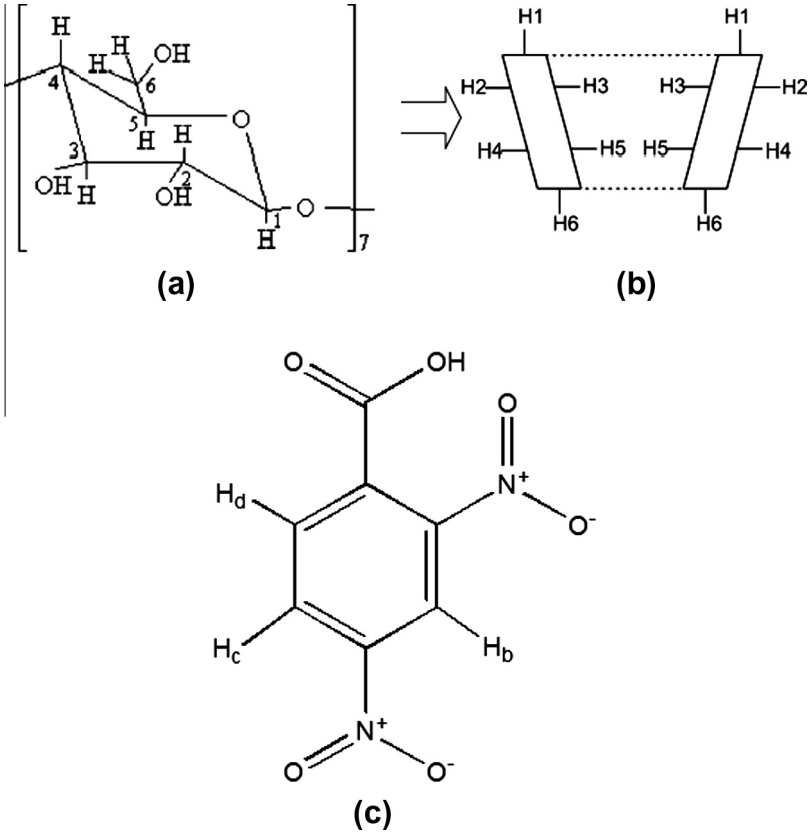

Scheme 7. (a) The stereo-configuration of β-CD and (b) truncated-cone of β-CD and (c) 2,4-DNB.

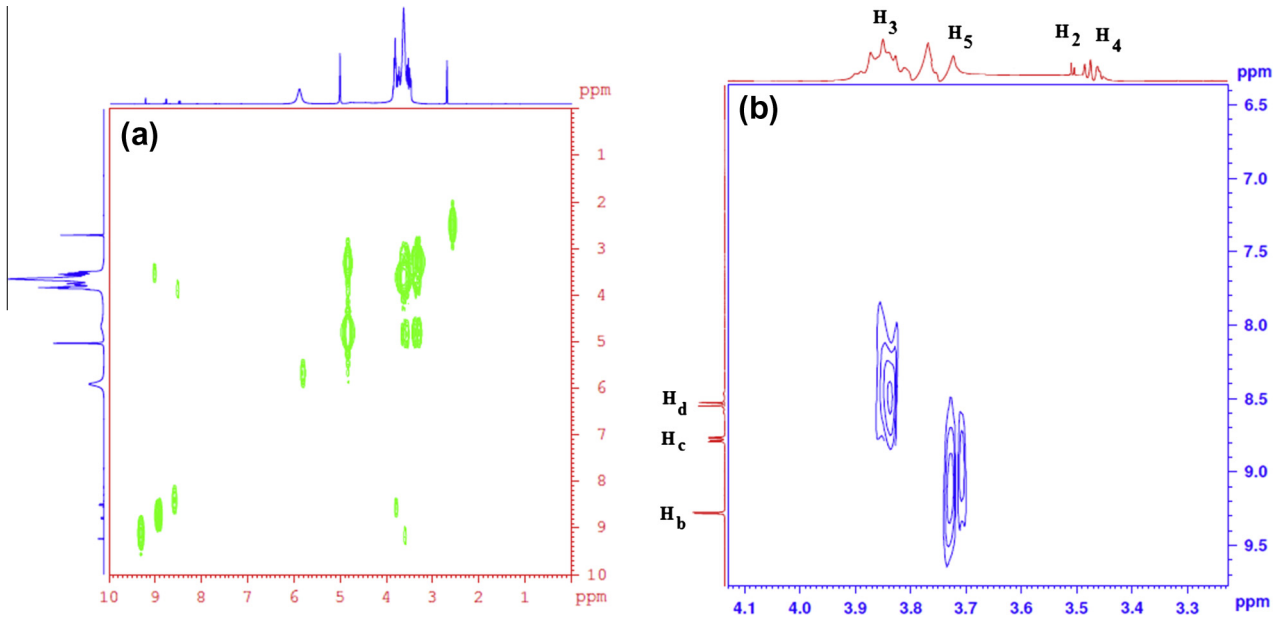

Fig. 7. The 2D ^{1}H NMR (ROESY) spectra of inclusion complex of (a) 2,4-DNB:β-CD, (b) Partial Counter plot of 2,4-DNB:β-CD in DMSO-d_6 at 300 K.

near of the upper rim of the β-CD. The characteristics of C—N (—NO_2) stretching vibration appeared at 835 cm^{-1} for 2,4-DNB and it shifted to 858 cm^{-1} for the inclusion complex also the intensity is reduced due to the nitro groups are included into the nanocavity of the β-CD. The characteristic peaks of —C=C— stretching appeared at 1618 cm^{-1} for 2,4-DNB and it shifted to 1631 cm^{-1} and the intensities is reduced due to the hydrophobic part of the benzene ring of 2,4-DNB were included in the nano cavity of the β-CD.

3.9. Powder X-ray diffraction pattern

The lack of crystallinity is an added evidence for the formation of inclusion complex [27]. Fig. 9 shows the XRD patterns for guest

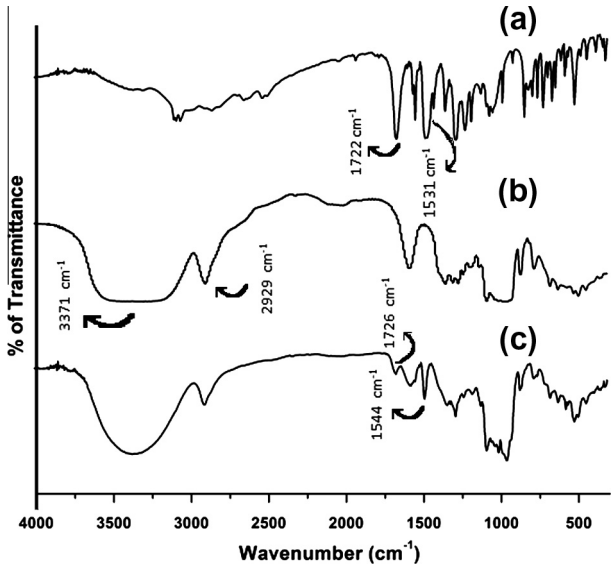

Fig. 8. FT-IR Spectra of (a) 2,4-DNB, (b) β-CD and (c) solid inclusion complex of 2,4-DNB:β-CD complex in KBr.

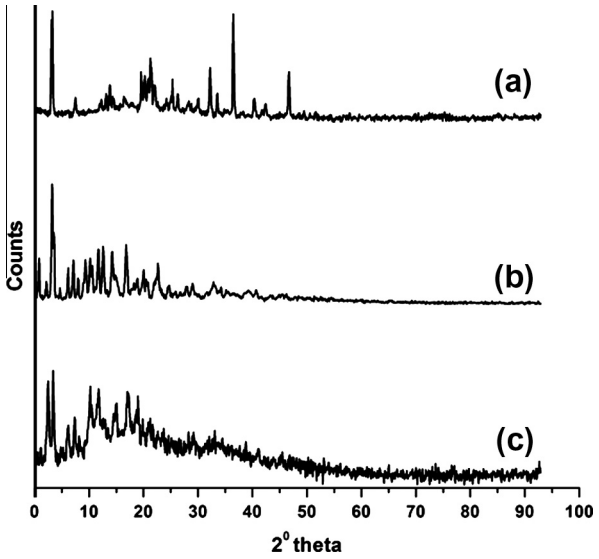

Fig. 9. Powder X Ray diffraction spectra of (a) 2,4-DNB, (b) β-CD and (c) solid inclusion complex of 2,4-DNB:β-CD.

(2,4-DNB), host (β-CD) and their complex systems were prepared by co-precipitation techniques at a molar ratio of 1:1. The powder X-ray diffraction pattern of 2,4-DNB (Fig. 9a) revealed that several sharp high intensity peaks at different diffraction angles (2θ) of 12.3, 20.3, 24.6, 25.1, 25.5, 25.9, 26.5, 28.9, 34.1, 35.1 and 37.3 suggesting that the 2,4-DNB existed as crystalline nature. The β-CD (Fig. 9b) showed a crystalline diffractogram, while a diffuse halo-pattern was recorded for 2,4-DNB-β-CD (Fig. 9c) demonstrating its amorphous nature. The diffraction patterns of the investigated in the complex correspond to the correct position of those of the pure components. The lower intensities of the diffraction peaks indicate that the particle sizes were reduced during complex preparation in solution phase of the pure crystalline components. Few of diffraction peaks of 2,4-DNB was matched with those off β-CD was evident. A typical diffuse pattern indicating the entirely amorphous nature of 2,4-DNB in complexed state.

3.10. Scanning electron microscope morphological observations

Scanning electron microscope (SEM) is well suited for visualizing the surface texture of the deposited film. The SEM analysis is ideal for quantitatively measuring the surface roughness and for visualizing the surface texture of the substance. First we observed surface morphological structure of (a) 2,4-DNB shows like a broken cement plate morphology, (b) β-CD shows as like a sheeted/bladed morphology (Fig. 10) by SEM, and then we also observed the surface morphological structure of (c) solid inclusion complex as like a milky white rectangular sheet morphology (Fig. 10c). These pictures clearly elucidated the difference of each other. Modification of crystals can be assumed as a proof of the formation of a solid inclusion complex with the nano hydrophobic cavity of β-CD.

4. Conclusions

The following conclusion can be arrived at from the above studies; the inclusion complex of 2,4-DNB with β-CD were prepared (aqueous and solid phases) and the structures of the complex were investigated by UV, ^{1}H NMR, 2D^{1}H NMR (ROESY), FT-IR, XRD and SEM techniques. The experimental results showed that the complex was the benzene ring part of the 2,4-DNB molecules was included into the β-CD cavity. Furthermore, the implementation of molecular modeling confirmed that the complex of 1:1 host–guest stoichiometry. The electrochemical study is also supporting evidence for the formation of inclusion complex. In addition, the prototropic reactions can be used to calculate the ground state acidity constant (p*K*a) values for the 2,4-DNB molecule by spectrophotometrically in the presence and absence of the β-CD.

Acknowledgements

One of the authors K. Srinivasan acknowledges to UGC-BSR for providing Research Fellowship for Science Meritorious (AU/UGC-BSR/IC/1069/2011) student.

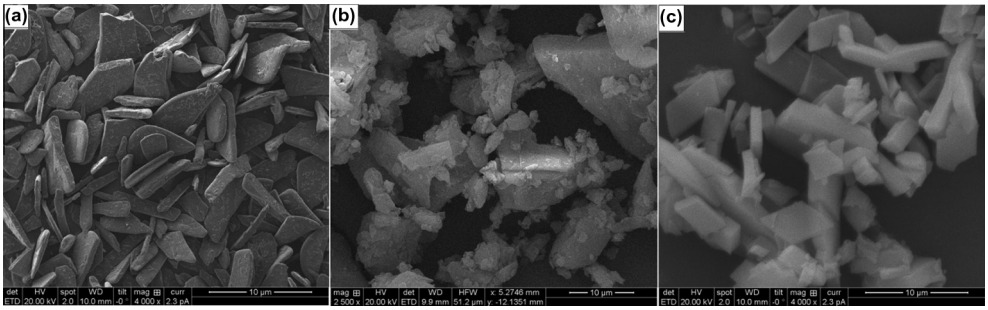

Fig. 10. Scanning electron microscope photographs (Pt. coated) of (a) 2,4-DNB, (b) β-CD and (c) solid inclusion complex of 2,4-DNB:β-CD.

Appendix A. Supplementary material

Supplementary data associated with this article can be found, in the online version, at http://dx.doi.org/10.1016/j.molstruc.2013.11.048.

References

[1] J. Szejtli, Chem. Rev. 98 (1998) 1743–1753.
[2] X.T. Shuai, F.E. Porbeni, M. Wei, I.D. Shin, A.E. Tonelli, Macromolecules 34 (2001) 7355–7361.
[3] A. Harada, T. Nishiyama, Y. Kawaguchi, M. Okada, M. Kamachi, Macromolecules 30 (1997) 7115–7118.
[4] G.M. Do Nascimento, J.E.P. Da Silva, S.I.C. De Torresi, P.S. Santos, M.L.A. Temperini, Mol. Cryst. Liq. Cryst. 53 (2002) 374–379.
[5] M.V. Rekharsky, Y. Inoue, Chem. Rev. 98 (1998) 1875–1917.
[6] H.J. Schneider, F. Hacket, V. Rudiger, Chem. Rev. 98 (1998) 1755–1786.
[7] L. Zhang, S. Lerner, W.V. Rustrum, G.A. Hofman, Bioelectrochem. Bioenerg. 48 (1999) 453–461.
[8] Y.L. Loukas, P. Jayasekera, G. Gregoriadis, Int. J. Pharm. 117 (1995) 85–94.
[9] Y.L. Loukas, V. Vraka, G. Gregoriadis, Int. J. Pharm. 144 (1996) 225–231.
[10] S.H. Choi, E. Nyongryu, J. Ryoo, K. Pillee, J. Inclusion Phenom. 40 (2001) 271–274.
[11] V. Stefano, B. Bruno, J. Chem. Therm. 41 (7) (2009) 880–887.
[12] H. Long, Y.X. Zhu, P.T. Kissinger, Chin. J. Anal. Chem. 31 (2003) 631–634.
[13] X. Guo, Z. Wang, S. Zhou, Talanta 64 (2004) 135–139.
[14] J.M. Chern, Y.W. Chien, Water Res. 36 (2002) 647–655.
[15] D.S. Duhovny, Y. Inbar, R. Nussinov, H.J. Wolfson, Nucl. Acids Res. 33 (2005) 363–367.
[16] M.L. Connolly, J. Appl. Crystallogr. 16 (1983) 548–558.
[17] C. Zhang, G. Vasmatzis, J.L. Cornette, C. DeLisi, J. Mol. Biol. 267 (1997) 707–726.
[18] G. Yagil, J. Phys. Chem. 71 (1967) 1034–1044.
[19] M.J. Jorgenson, D.R. Hartter, J. Am. Chem. Soc. 85 (1963) 878–883.
[20] K. Srinivasan, J. Vaheethabanu, P. Manisankar, T. Stalin, J. Mol. Struct. 987 (2011) 214–224.
[21] K. Srinivasan, K. Kayalvizhi, K. Sivakumar, T. Stalin, Spectrochim. Acta A 79 (2011) 169–178.
[22] M. Shanmugam, D. Ramesh, V. Nagalakshmi, R. Kavitha, R. Rajamohan, T. Stalin, Spectrochim. Acta Part A Mol. Biomol. Spectrosc. 71 (2008) 125–132.
[23] H.A. Bensi, J.H. Hildebrand, J. Am. Chem. Soc. 71 (1949) 2703–2707.
[24] G. Gaitano, P.R.S. Rozas, J.R. Isasi, A.G. Martínez, G. Tardajos, J. Phys. Chem. B 108 (2004) 14154–14162.
[25] T. Sohajda, S. Beni, E. Varga, R. Ivanyi, A. Racz, L. Szente, B. Noszal, J. Pharm. Biomed. 50 (2009) 737–745.
[26] H.Y. Wang, J.H. Feng, Y.L. Pang, Spectrochem. Acta, Part A 65 (2006) 100–105.
[27] R.O. Williams, V. Mahaguna, M. Sriwongjanya, Eur. J. Pharm. Biopharm. 46 (1998) 355–360.